FLIGHT TRAJECTORY TRACKING FOR A HELICOPTER IN TAIL ROTOR FAILURE

Yusuf Onur Arslan, Turkish Aerospace, Ankara, Turkey
Ilgaz Doğa Okcu, Turkish Aerospace, Ankara, Turkey

Abstract

A helicopter in tail rotor failure that cannot perform emergency landing due to lack of available landing area is under investigation. In the previous study, flight trajectories for a helicopter in tail rotor failure were generated for different scenarios. In this work, the trajectory optimization process is enhanced and trajectory tracking is achieved by linear and nonlinear simulations. For the study, the generic helicopter model in FLIGHTLAB is used and a tail rotor failed model is created. The path generation process is performed offline in MATLAB with an open-source trajectory optimization tool, OptimTraj. The trajectories are obtained by making improvements in the definitions of optimization constraints and in the linear models. The trajectories are given as a reference to the tracking controllers and the simulations are performed. For nonlinear simulations, real-time module of FLIGHTLAB is utilized and the run-time model and the controller which are in separate environments are interconnected.

1. INTRODUCTION

In a conventional helicopter, the tail rotor is the primary component creating the necessary anti-torque to balance main rotor torque. Especially for low speed flight, the tail rotor is the sole anti-torque creator whereas, during high speed, the vertical fin of the helicopter can contribute to anti-torque as well. That is why a tail rotor failure (TRF) can have catastrophic consequences especially at low speed regimes. Recommended emergency procedure for a TRF is almost always to autorotate. Autorotation, normally utilized during engine failures since the main rotor is deprived of the torque necessary for rotation, is the perfect solution for a helicopter which has lost its primary anti-torque generating component, the tail rotor. Since there is no net torque on the main rotor during autorotation there is also no need for an anti-torque source (Ref. 1). However, for an autorotation a helicopter needs to have a sufficient height-above-ground and a suitable safe landing zone, one of which may not be available during a TRF. In such an unlikely condition, it may still be possible to maneuver the helicopter utilizing the anti-torque generated by the vertical fin, to find a suitable landing spot or to gain altitude for an autorotational landing.

In this work, although trajectory tracking for a helicopter in TRF is the main subject of interest, trajectory generation is also studied and the flight paths are improved. In case of TRF, pedal control authority would be lost. Therefore, directional controllability of the helicopter reduces considerably. Instead of pedal control, the rate of change of main rotor speed is utilized for directional control during this study. Using the change of rotor speed as a pilot input is assumed to be possible due to engine throttle. Even though the throttle is not among the main pilot inputs, it is a way to change the exerted torque on the main rotor; hence, manipulating the rotor speed. Especially for older helicopters, the throttle which was mounted at the end of the collective lever could be controlled by pilots. However, in today's helicopters, this input is controlled by an engine controller. That is, the throttle can be a solution for increasing or decreasing the rotor speed for engine-powered flights. Although throttle can be used to increase the rotor speed in autorotation, it cannot be used to decrease the speed. For this case, a mechanism that decreases the kinetic energy of the rotor must be suggested. Applying collective control would increase drag force on the blades while it increases the lift. However, it cannot be a good solution for cases that require low collective and low rotor speed at the same time in a trajectory. In order to solve this problem, a rotor brake is proposed to decrease the rotor speed in autorotation. In fact, the rotor brake is used in helicopters but after the helicopter lands and the engines are shut down. In this study, the existence of a sophisticated rotor brake is assumed to decrease the rotor speed when it is necessary. It should be emphasized that the throttle and the rotor brake are controlled by the tracking controller.

In order to generate flight trajectories, an open-source trajectory optimization tool, OptimTraj, is utilized. OptimTraj can solve a trajectory optimization problem by the direct collocation method by defining an objective function, system dynamics, path constraints, and boundary constraints (Ref. 2). In order to reduce the computation time, this work utilizes linear helicopter models to represent the system dynamics. Several linear models, generated around selected equilibrium points, are utilized and the numbers that belong to the linear models are interpolated to form the most representative model and cover each point in state-space during the flight trajectory optimization. The linear helicopter models are created by linearizing the generic model in FLIGHTLAB around the trim points in level flight at 100 knots, left and right bank turns at 100 knots, and in autorotation at 60 and 80-knot conditions. Two different cases are inspected for trajectory generation. In the first case, a path is generated for a helicopter at high speed and it is in level forward flight trim with a TRF to proceed to a predefined location in space. In the second case, a trajectory is generated so that a helicopter at low speed in an autorotational descent trim with a TRF can accelerate to a level forward flight.

After the flight paths are obtained, in order to follow the generated trajectories, tracking controllers are developed. An inversion based controller is utilized for position tracking and an LQI controller is designed for state tracking. The controllers are tested with linear and nonlinear model simulations. For nonlinear model simulations, FLIGHTLAB run-time model is utilized in conjunction with SIMULINK. The helicopter response to TRF itself is not included in the trajectory generation and tracking process in this study.

2. LITERATURE SURVEY

For the study, a detailed literature survey is conducted. Most related studies are summarized in this part.

Yomchinda et al. (Ref. 3) performed path planning for an unmanned helicopter in engine failure during autorotation. The landing point is specified and the computed trajectory is followed by a controller until landing. Chowdhary et al. (Ref. 4) succeeded to guide a fixed-wing UAV under actuator failure and structural damage on one wing. The flight path is defined by waypoints. The commands are used by an outer-loop linear controller to generate feasible attitude commands. The inner-loop attitude control is achieved by using either a linear attitude controller or a neural network-based model reference adaptive controller. GT Twinstar UAV is used for flight tests. Bottaso et al. (Ref. 5) performed planning and tracking of trajectories for the simulation of maneuvers with multibody models. A maneuver is defined as an optimal control problem. This definition becomes the input for a planning layer that determines the helicopter trajectory by solving the optimization problem for a reduced model. The resulting trajectory feeds into a control layer, which tracks the computed optimal path using a non-linear model predictive formulation and steers the multibody model accordingly. Garcia et al. (Ref. 6) presented a fuzzy controller capable of waypoint navigation under tail rotor failure on a small unmanned helicopter. In the study, the helicopter is navigated while it is spinning due to lack of anti-torque. Both loss of tail rotor and tail actuator lockout cases are investigated. Budiyono and Wibowo (Ref. 7) designed an optimal tracking controller for the R-50 helicopter model to follow predefined trajectories. LQR method is utilized with the presence of input constraints for path following. Abbeel et al. (Ref. 8) presented the first autonomous controller to successfully pilot an RC helicopter during an autorotation descent and landing. Differential dynamic programming is utilized to design the controller. The flight tests are conducted with the XCell Tempest helicopter.

Although there are many studies for trajectory generation, autorotation, path following, and TRF in helicopters, a study that covers all these subjects combined is absent from the literature to the writers' knowledge. In the previous work, flight trajectories were generated for a helicopter in TRF (Ref. 9). The suggestion was that a helicopter in TRF does not have to autorotate when landing is not safe. It can fly to a certain position where autorotation could be performed safely. The case that brings the helicopter from autorotation to level flight is also studied. These scenarios are depicted in Figure 1. Additionally, in the absence of pedal input, the change of main rotor speed is proposed to achieve the directional control of the helicopter in TRF. Original contributions of this study is the actual tracking of the generated flight trajectories by a controller and investigating additional failure scenarios.

Figure 1: Possible actions in TRF

3. HELICOPTER MODEL

A generic nonlinear model similar to Sikorsky UH-60A in FLIGHTLAB is utilized for the study. Trim points are searched for TRF condition for different speeds and linear models are generated for system dynamics. In order to reduce complexity and to be able to focus on the open-loop system, horizontal tail controller, SAS and pitch bias controller are switched off and the mechanical mixing of pilot controls is eliminated from the default nonlinear model. Tail rotor failure can be injected in the generic model by a switch; thus, all force and moments produced by the tail rotor are terminated.

The previous work (Ref. 9) focused on the scenarios for a helicopter at 80 knots because the helicopter can be trimmed in level flight for 80 knots and above. The vertical tail is sufficient by itself at and above 80 knots. However, at this speed, helicopter characteristics may suddenly change because of the TRF. In addition, Ref. 10 states that the recommended autorotation speed is 80 knots for UH-60A. Hence, maneuvering from autorotation at 80 knots to level flight at 100 knots would be reasonable. Therefore, in this work, scenarios for a helicopter at 100 knots are investigated to leave a speed margin. For the high speed case, the aim is to navigate the helicopter to a final position. Therefore, turning maneuvers will be required to arrive at the specified location. Hence, left and right coordinated turns at 100 knots are included to the linear model set. Also, for the trajectory that brings the helicopter from autorotation to level flight condition, linear models for autorotation at 60 and 80 knots are created and added to the linear model set.

For the linear model, the states and controls are given as,

(1) $$x = [\Omega \; \phi \; \theta \; u \; v \; w \; p \; q \; r]^T$$

(2) $$u = \left[\delta_{col} \; \delta_{lon} \; \delta_{lat} \; \delta_{ped} \; \dot{\Omega}\right]^T$$

Note that pedal control has no effect on the helicopter during TRF condition. Therefore, main rotor acceleration is added into the controls and the main rotor speed is added into the states so that the directional control of the helicopter could be enhanced.

While the linear models are used in controller design and in the trajectory generation process in order to reduce complexity and to get results rapidly, the nonlinear model is used for the tracking simulations. The controller is developed in SIMULINK environment. Therefore, the Run-time System is utilized in order to communicate the model with the controller.

A black-box model, called FCM model is generated in FLIGHTLAB. The FCM model is driven by SIMPHONY module of FLIGHTLAB. The generated black-box model can be interfaced with external systems such as SIMULINK. A C-script is prepared for driving the FCM model and for input-output signal regulation. It transfers the data to the shared memory of SIMPHONY. UDP communication protocol is implemented in a C-script and IP/Port numbers are provided according to IP/Port numbers in UDPsend and UDPreceive blocks in SIMULINK. MATLAB-FLIGHTLAB connection is simply schematized in Figure 2.

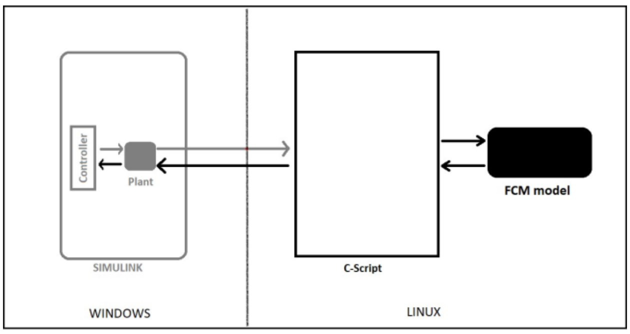

Figure 2: MATLAB-FLIGHTLAB connection diagram

4. TRAJECTORY GENERATION

Flight paths are found by using OptimTraj. Final position or final state of the helicopter in TRF is defined as a constraint to the program along with the objective function and state bounds. For high speed case, final position of the helicopter is aimed and three maneuvers are selected for trajectory generation: right turn, left turn and climb. It is observed that the helicopter can complete the objected turn maneuvers; however, it has struggled to achieve the point that needs a climb. This is simply because the system dynamics of the helicopter in TRF does not permit to make a sharp climb. Therefore, a lower point is chosen to demonstrate the climb maneuver.

The system dynamics used in the trajectory optimization problem are provided by interpolating the linear models according to the distance of the current states to the equilibrium points of the linear models in state space. Thus, the validity of the system dynamics is expanded so that different flight conditions can be covered during optimization.

For position navigation in level flight at high speed case, the minimum control objective function is implemented. For the transitions from autorotation to level flight at low speed case, minimum altitude descent is implemented as the objective function; hence, the minimum allowable height from the ground for TRF can be estimated.

For minimum control,

(3) $$\min_{t_0, t_F, x(t), u(t)} \int_{t_0}^{t_F} u(\tau)^2 d\tau$$

For minimum descent,

(4) $$\min_{t_0, t_F, x(t), u(t)} \int_{t_0}^{t_F} z_i\big(\tau, x(\tau), u(\tau)\big)^2 d\tau$$

Flight path optimization problem is summarized in Table 1. Note that in all scenarios, the trajectory grid number is chosen as 100.

Trajectory generation is the main focus in the previous work (Ref. 9). Much more detailed explanation can be found there. After obtaining the trajectory as off-line, it is given as a reference to the controller for tracking.

Table 1: Summary of path optimization information

Scenario	Failure Cond.	Linear Models	Objective Func.	Constraints
Scenario 1	High speed	100 kt level flight 100 kt right turn 100 kt left turn	Minimum control	Final Position Sys. Dynamics State Bounds
Scenario 2	High speed	100 kt level flight 100 kt right turn 100 kt left turn	Minimum control	Final Position Sys. Dynamics State Bounds
Scenario 3	High speed	100 kt level flight 100 kt right turn 100 kt left turn	Minimum control	Final Position Sys. Dynamics State Bounds
Scenario 4	Low speed	60 kt autorot. 80 kt autorot.	Minimum descent	Sys. Dynamics State Bounds
Scenario 5	Low speed	80 kt autorot. 100 kt level flight	Minimum descent	Sys. Dynamics State Bounds

5. TRACKING CONTROLLER

In this paper, two control methods are implemented in order to achieve trajectory tracking of a helicopter in TRF. The problem is handled in two scenarios as in the trajectory generation. The first one is high speed case and the position tracking is achieved by an inversion based controller. Dynamic inversion for the outer loop and linear model inversion for the inner loop are efficient and suitable methods for position tracking (Ref. 3)(Ref. 11). The second one is low speed case and LQI method (Ref. 12) is selected for the state tracking. The linear models are interpolated to approximate the current state of the helicopter in order to increase the controller performance.

5.1. Inversion Based Controller (IBC)

Inversion based controller is developed in a cascade form. It consists of an inner and an outer loop. Main objective of the inner loop is to track the generated Euler angles and the total acceleration. On the other hand, the outer loop is responsible for tracking the position references. The block diagram of the control system developed in SIMULINK is depicted in Figure 3.

Rotational states are controlled in the inner loop by using the linear model inversion method. It is assumed that cyclic and pedal are responsible for the attitudes and collective is responsible for the total acceleration of a helicopter under nominal conditions (Ref. 13). However, in this study, instead of the pedal, the derivative of the speed of main rotor is utilized for the directional control of a helicopter in TRF.

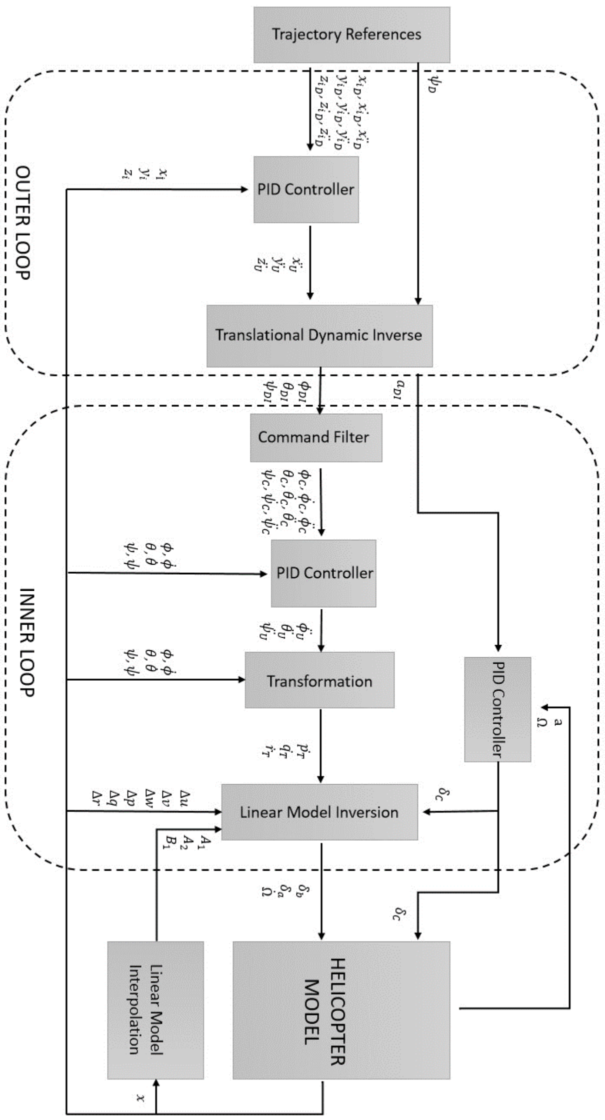

Figure 3: Block diagram of inversion based control system

In the transformation block, by using Eq. (5), Eq (6) and Eq. (7), the Euler angles and their first and second derivatives are transformed into body angular accelerations. The Euler angles and their first derivatives are the model outputs; whereas, the second derivatives come from the PID block. The outputs of the transformation block which are the body angular accelerations are the command signals for the linear model inversion block.

(5) $$\dot{p} = \ddot{\phi} - \ddot{\psi}\sin\theta - \dot{\theta}\dot{\psi}\cos\theta$$

(6) $$\dot{q} = \ddot{\theta}\cos\phi - \dot{\phi}\dot{\theta}\sin\phi + \ddot{\psi}\sin\phi\cos\theta + \dot{\phi}\dot{\psi}\cos\phi\cos\theta - \dot{\theta}\dot{\psi}\sin\phi\sin\theta$$

(7) $$\dot{r} = -\ddot{\theta}\sin\phi - \dot{\phi}\dot{\theta}\cos\phi + \ddot{\psi}\cos\phi\cos\theta - \dot{\phi}\dot{\psi}\sin\phi\cos\theta - \dot{\theta}\dot{\psi}\cos\phi\sin\theta$$

In the the linear model inversion block, rotational and translational states are decoupled. The linear model used in this study contains a 9-by-9 system matrix and a 9-by-5 control matrix. The decoupled system is given in Eq. (8) in state-space representation where x_1 contains the body rates, x_2 contains the body velocities and collective input, A_1 is the stability matrix that contains the effects of rotational states on themselves, A_2 is the stability matrix that contains the effects of translational states on rotational states, B_1 is the control matrix that contains the effects of controls on rotational states, and finally, u_1 contains longitudinal cyclic, lateral cyclic and rotor speed input. Collective is added to x_2 vector as a slow translational state because its dynamic effect is slower than the other controls (Ref. 14).

(8) $$\dot{x_1} = A_1x_1 + A_2x_2 + B_1u_1$$

(9) $$x_1 = [p, q, r]^T$$

(10) $$x_2 = [u, v, w, \delta_c]^T$$

(11) $$u_1 = [\delta_b, \delta_a, \dot{\Omega}]^T$$

By manipulating Eq. (8), u_1 can be found as,

(12) $$u_1 = B_1^{-1}(\dot{x_1} - A_2x_2 - A_1x_1)$$

In the second branch of the inner loop, desired total acceleration which is generated by the outer loop is used in order to produce collective input. The vertical component of the thrust vector of the main rotor is the main contributor of the helicopter total acceleration. Therefore, relating collective with the total acceleration is a very reasonable idea. The acceleration command is processed in the collective controller by using the acceleration which is calculated from the model outputs as feedback signal. The calculation of the helicopter acceleration is given in Eq. (13) where L_{EB} is the transformation matrix from body-fixed reference frame to Earth-fixed reference frame. Note that the commanded acceleration is given in inertial frame; therefore, body acceleration of the helicopter is transformed.

(13) $$\begin{bmatrix} a_{x_i} \\ a_{y_i} \\ a_{z_i} \end{bmatrix} = L_{EB}\left(\begin{bmatrix} \dot{u} \\ \dot{v} \\ \dot{w} \end{bmatrix} + \begin{bmatrix} 0 & -r & q \\ r & 0 & -p \\ -q & p & 0 \end{bmatrix}\begin{bmatrix} u \\ v \\ w \end{bmatrix}\right) - \begin{bmatrix} 0 \\ 0 \\ g \end{bmatrix}$$

The collective controller is composed of a PI controller and a P controller. While PI controller processes the acceleration error signal, the P controller processes the error signal of main rotor speed. P controller for the rotor speed is added in order to prevent too high or too low rotor speed values. Thus, input effort on the rotor speed is passed to the collective. The block diagram of the collective controller is shown in Figure 4.

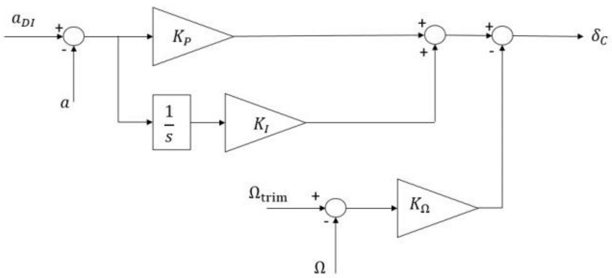

Figure 4: Block diagram of the collective controller

The inertial positions are controlled in the outer loop. It receives the position and heading references found by OptimTraj and generates roll, pitch and acceleration commands to the inner loop. Heading angle reference is directly passed to the inner loop without any change. In the outer loop, a command filter is not used. The necessary derivatives of inertial positions are calculated offline and given as reference signals to the PID block.

In translational dynamic inverse, it is assumed that the body accelerations in x and y-directions are assumed to be small compared to body acceleration in z-direction. Hence, by using Eq. (14), the desired roll and pitch angles can be calculated (Ref. 13). The translation dynamic inverse block composes Eq. (15), Eq. (16) and Eq. (17).

(14) $$\begin{bmatrix} a_{x_i} \\ a_{y_i} \\ a_{z_i} - g \end{bmatrix} = L_{EB} \begin{bmatrix} a_{x_b} \\ a_{y_b} \\ a_{z_b} \end{bmatrix}$$

(15) $$a = \sqrt{a_{x_i}^2 + a_{y_i}^2 + \left(a_{z_i} - g\right)^2}$$

(16) $$\phi \approx \sin^{-1}\left(\frac{-a_{x_i}\sin\psi + a_{y_i}\cos\psi}{a_{total}}\right) + \phi_{trim}$$

(17) $$\theta \approx \tan^{-1}\left(\frac{-a_{x_i}\cos\psi + a_{y_i}\sin\psi}{a_{z_i} - g}\right) + \theta_{trim}$$

5.2. LQI Controller

Linear quadratic regulator with integral action is implemented to track the helicopter states. It is an optimal solution for tracking states of a linear system in which the performance index in Eq. (18) is minimized. It consists of a state feedback gain set and a feedforward integral gain set. The block diagram of the control system is depicted in Figure 5.

(18) $$J = \int_0^\infty (x^T Q x + u^T R u)dt$$

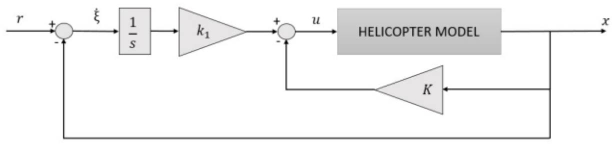

Figure 5: Block diagram of LQI control system

The optimal gains are found by using,

(19) $$K = R^{-1}B^T P$$

Where P is a positive-definite matrix that results from Riccati equation,

(20) $$A^T P + PA - PBR^{-1}B^T P + Q = 0$$

The matrices of the resulting regulator are given by,

(21) $$\hat{A} = \begin{bmatrix} A & 0 \\ -C & 0 \end{bmatrix} \qquad \hat{B} = \begin{bmatrix} B \\ 0 \end{bmatrix}$$

The solution of Eq. (20) would give the gains in the form of,

(22) $$\hat{K} = [K \quad -k_1]$$

Where K is the gain set for the stabilization and k_1 is the gain set for the integral action. Hence, the closed-loop system can be written by (Ref. 15).

(23) $$\begin{bmatrix} \dot{x} \\ \dot{\xi} \end{bmatrix} = \begin{bmatrix} A - BK & Bk_1 \\ -C & 0 \end{bmatrix} \begin{bmatrix} x \\ \xi \end{bmatrix} + \begin{bmatrix} 0 \\ 1 \end{bmatrix} r$$

(24) $$y = [C \quad 0] \begin{bmatrix} x \\ \xi \end{bmatrix}$$

Note that the system is full state feedback and ξ represents the selected states for tracking. The input is given by,

(25) $$u = -[K \quad -k_1] \begin{bmatrix} x \\ \xi \end{bmatrix}$$

Since the utilized linear models are different for each scenario, the weighting matrix for state error, Q, and the weighting matrix for the input effort, R, are determined for each case. Furthermore, tracked states differ for each scenario because deviation of states that defining the maneuver is more important. For 60-knot autorotation to 80-knot autorotation transition, tracked states are selected as u, w, ϕ and θ. On the other hand, for 80-knot autorotation to 100-knot level flight transition, tracked states are selected as u, v, ϕ and θ. In level flight trim, the helicopter needs a large sideslip angle in order to produce the required anti-torque. Therefore, in this scenario, the lateral velocity is needed to be selected for tracking. In addition, the forward velocity plays an essential role for directional stability. As the helicopter is faster, the effect of the vertical fin is higher. Therefore, it is kept in selected states for tracking.

6. RESULTS AND DISCUSSION

The results show that the helicopter in TRF can be navigated to a predefined location or it can be brought to a new flight condition. Of course, the anticipated location or trim condition must be a sensible option so that the helicopter really can achieve the aim.

In this work, flight trajectory of a helicopter under TRF is calculated and these trajectories are followed by a fully autonomous controller in five example scenarios. It is assumed that landing immediately is not possible and a landing area is far away. If the helicopter has sufficient forward speed, it is shown that it can fly in level with sideslip. For this case, a point in space is specified to navigate the helicopter and the flight trajectory is obtained for minimal input usage. If the forward speed is low, the trajectory that brings the helicopter from autorotation to level flight is obtained. For this case, minimum altitude descent is aimed. For all scenarios, it is assumed that the helicopter is already in trim condition at the beginning. The investigated flight scenarios are summarized in Table 2.

Table 2: Summary of investigated flight scenarios

Scenario	Maneuver Definition	Controller
Scenario 1	Right turn at 100 kt	IBC
Scenario 2	Left turn at 100 kt	IBC
Scenario 3	Climb at 100 kt	IBC
Scenario 4	60 kt autorot. to 80 kt autorot.	LQI
Scenario 5	80 kt autorot. to 100 kt level flight	LQI

For each case, results are represented to illustrate the generated flight path and the nonlinear simulation tracking. Note that the helicopter is initially at [0, 0, 3000] ft and it is shown by 'o' mark; whereas the end position is marked with 'x'.

In Scenario 1, the helicopter in level flight at 100 knots is commanded to right turn maneuver without an altitude change. The desired terminal position is specified as [5000, 2500, -3000] ft in order to demonstrate the right turn maneuver capability. The resulting flight path is shown in Figure 6. While the final position of the helicopter is found as [4997, 2505, -3000] ft in the optimization result, the simulation results is [5013, 2476, -2895] ft. It can be stated that the nonlinear model could follow the referenced trajectory successfully. In Figure 7, it can be noticed that OptimTraj and IBC need to change the rotor speed in the same way to track the heading reference. Figure 8 indicates that the helicopter rolls right to initiate the maneuver; and, after flying for a while with a positive roll, it returns the wings- level. Although the roll and pitch angles are not given as a reference to the nonlinear model, the simulation results are very close to the optimal angle values.

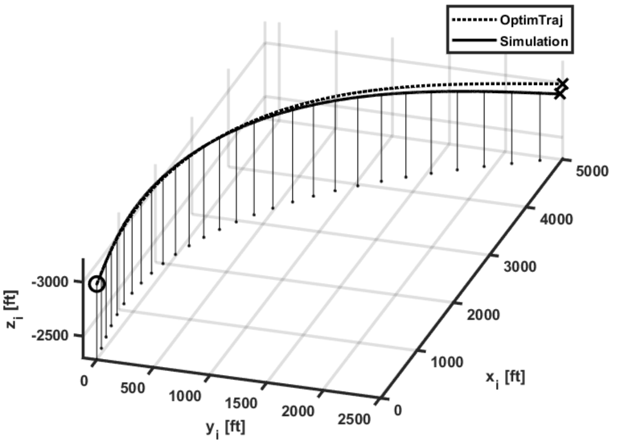

Figure 6: Scenario 1 – Position trajectory

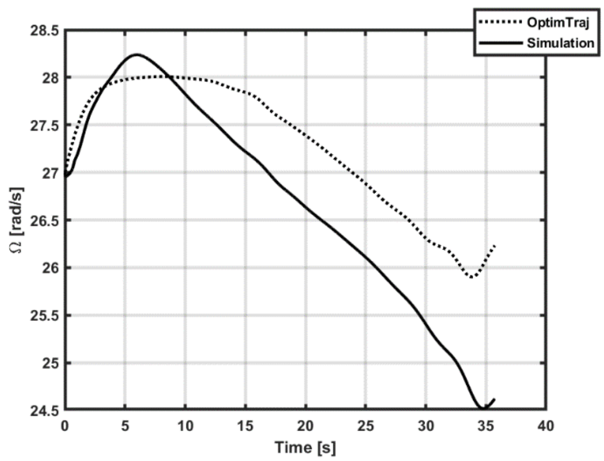

Figure 7: Scenario 1 – Main rotor speed

In Scenario 2, the helicopter in level flight at 100 knots is maneuvered to the final inertial position of [5000, -2500, -3000] ft. The flight trajectory is plotted in Figure 9. OptimTraj finds the terminal position as [4999, -2502 0] ft. On the other hand, the simulation result is [5046 -2498 -2908] ft. It can be stated that the nonlinear model could follow the referenced trajectory successfully.

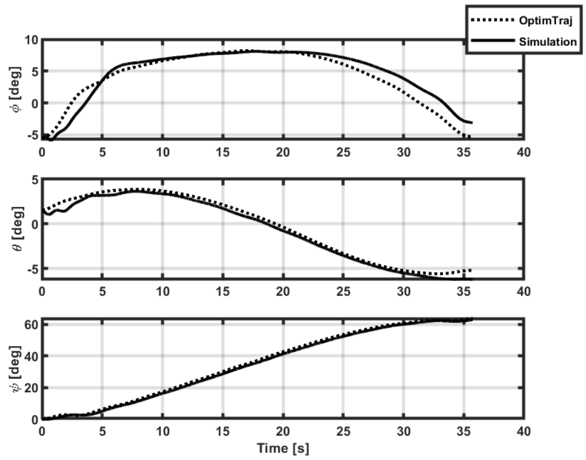

Figure 8: Scenario 1 – Euler angles

In Scenario 3, the helicopter in level flight at 100 knots is commanded to demonstrate the climb maneuver capability without a lateral position change. The desired terminal position is specified as [5000, 0, -3400] ft. The flight trajectory is plotted in Figure 10. While the final position of the helicopter is found as [5000, 10, -3400] ft in the optimization result, the simulation results is [5043, -39, -3242] ft. It can be noticed that the nonlinear model is struggled to climb the desired point. The source of the difference could be the absence of a linear model for climb condition. In this scenario, climb rate of the helicopter can be estimated as 500 ft/m. Figure 11 shows the change of the main rotor speed. It is seen that the optimal solution and the controller need to increase the rotor speed to climb the aimed point without lateral shift.

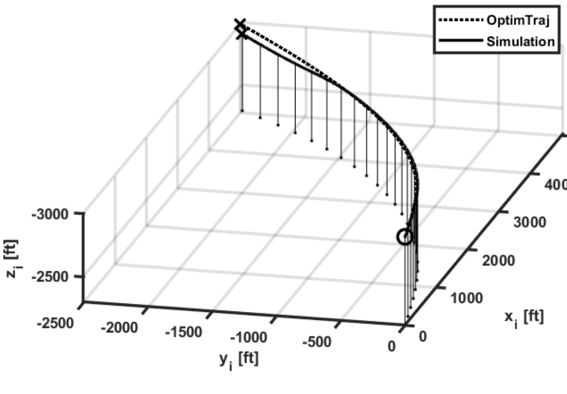

Figure 9: Scenario 2 – Position trajectory

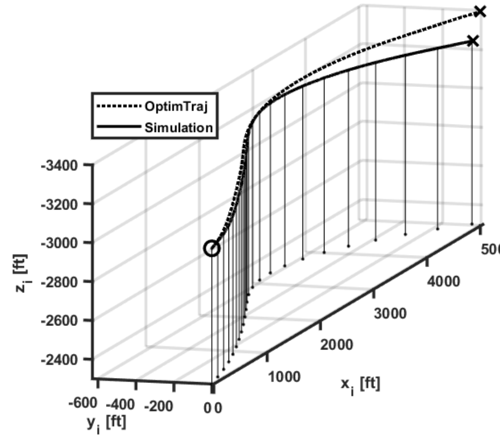

Figure 10: Scenario 3 – Position trajectory

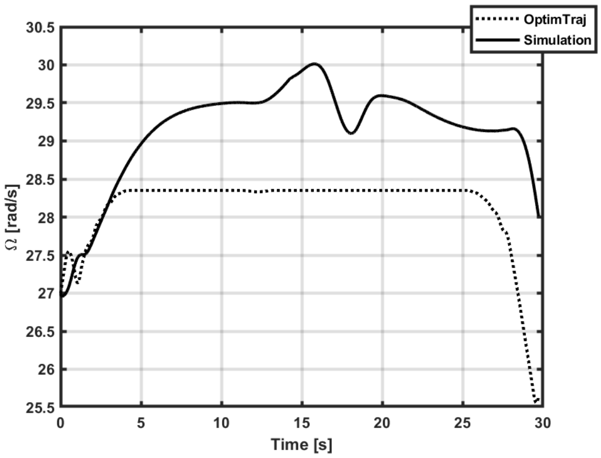

Figure 11: Scenario 3 – Main rotor speed

In Scenario 4, the transition of the helicopter from autorotation at 60 knots to autorotation at 80 knots is investigated. Figure 12 shows the linear model transition through the path. In order to quantify the closeness of the current state of the helicopter to the linear models by the states, which have different unit, weighting is performed. The weights are chosen according to their unit and their effectiveness on the maneuver. It can be noticed that optimal solution reaches the objected trim condition almost perfectly. In the nonlinear simulation, the helicopter reaches 80-knot autorotation trim with a small error. Figure 13 demonstrates the flight trajectory of the helicopter through the transition. Note that OptimTraj estimates that the helicopter needs 566 ft vertical distance for this maneuver. However, the simulation shows that the helicopter needs 668 ft.

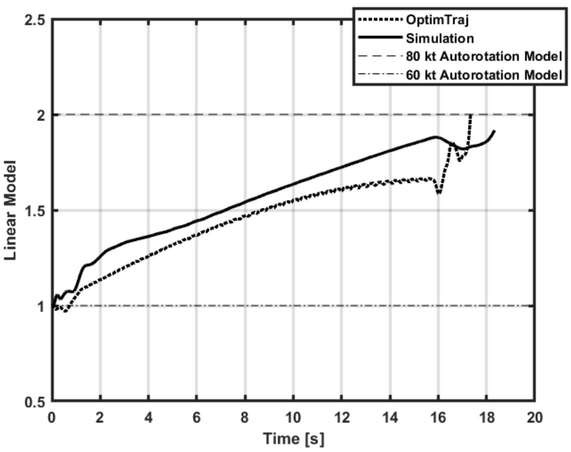

Figure 12: Scenario 4 – Linear model transition

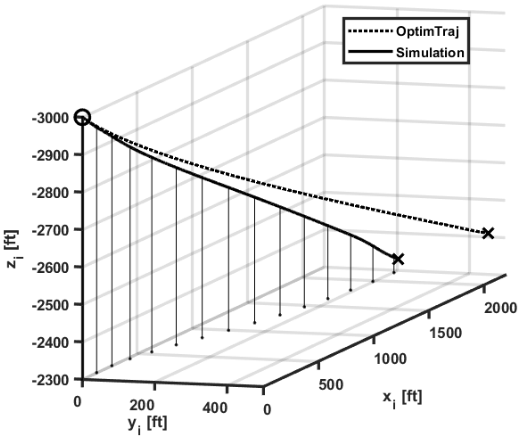

Figure 13: Scenario 4 – Position trajectory

In Scenario 5, the transition of the helicopter from autorotation at 80 knots to level flight at 100 knots is obtained. The model transition can be seen in Figure 14. Although there is a small error in the simulation, the linear model transforms from 1 to 2 indicating that the helicopter in autorotation trim at 80 knots completes the trajectory by achieving level flight at 100 knots. Since the helicopter in TRF cannot be in level without a large sideslip angle, both OpimTraj and the LQI controller tries to create it. This can be seen in Figure 15 with the airspeed and angle of attack change. It can be noticed that the air data parameters of the nonlinear model behave very closely to the optimal solution. Figure 16 shows the flight trajectory of the helicopter through the transition. Note that OptimTraj estimates that the helicopter needs 21 ft vertical distance for this maneuver. However, the simulation shows that the helicopter needs 273 ft in order to achieve level flight trim.

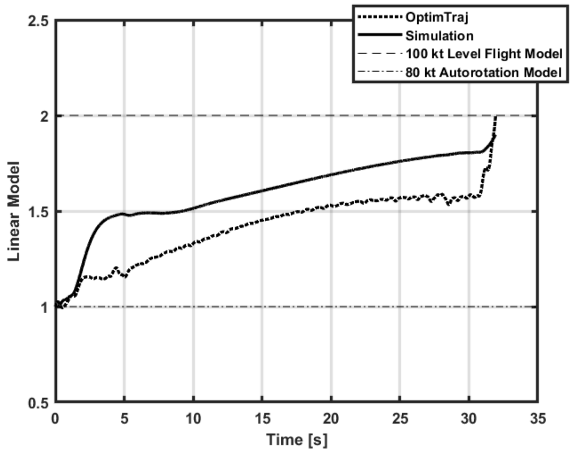

Figure 14: Scenario 5 – Linear model transition

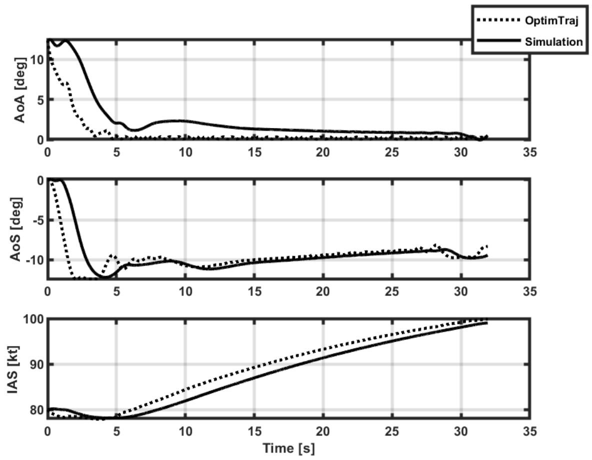

Figure 15: Scenario 5 – Air data parameters

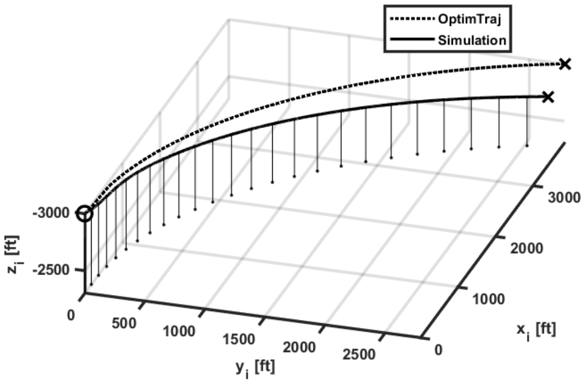

Figure 16: Scenario 5 – Position trajectory

7. CONCLUSIONS

The results show that in TRF condition, level flight and autorotation, of course, are possible in a helicopter depending on its forward velocity. If the helicopter has enough forward speed, it can be stabilized in level flight condition thanks to its vertical fin. However, if the forward speed is low, the helicopter can be stabilized with autorotative flight.

For directional control, changing the main rotor speed is utilized because of the absence of the pedal control. In addition, rotor speed is added to the state matrix in the linear models to represent its effect.

In this paper, trajectory tracking of a helicopter in TRF is performed. The results of position tracking and the results of trim condition transition are presented with five example scenarios. In high speed case, the helicopter is guided with position and heading reference to a desired terminal point by using an inversion based controller. In low speed case, the trim transition is performed with selected state references by an LQI controller. The results are obtained by using nonlinear helicopter model and compared with the optimal solution. It can be stated that:

1. The helicopter follows the position references and achieves the target positions with a small error. Furthermore, the helicopter could successfully move from one trim condition to another.
2. Using the change of the main rotor speed as a control increases directional control of the helicopter. Its practical implementations and results should be investigated and analyzed.
3. The necessary altitude for the helicopter to be able to stay in the air when a tail rotor failure occurs can be estimated.
4. With this approach, different target points can be experimented in order to map the maneuver capability of a helicopter in tail rotor failure condition.
5. Different control methods should be implemented in order to enhance the tracking performance of the nonlinear model.

Author contact:

Yusuf Onur Arslan yusufonur.arslan@tai.com.tr

Ilgaz Doğa Okcu iokcu@tai.com.tr

8. REFERENCES

1. Johnson, W., *Rotorcraft Aeromechanics*, Cambridge University Press, New York, NY, 2013, pp. 105.
2. Kelly, M., "An Introduction to Trajectory Optimization: How to Do Your Own Direct Collocation," *SIAM Review*, no. 59, pp. 849-904, Jan. 2017.
3. Yomchinda, T., Horn, J. F. and Langelaan, J. W., "Autonomous Control and Path Planning for Autorotation of Unmanned Helicopters," American Helicopter Society 68th Annual Forum Proceedings, Fort Worth, TX, May 2012.
4. Chowdhary, G., Johnson, E. N., Chandramohan, R., Kimbrell, M. S. and Calise, A., "Guidance and Control of Airplanes Under Actuator Failures," *Journal of Guidance, Control, and Dynamics*, Vol. 36, (4), 2013, pp. 1093–1104. DOI: 10.2514/1.58028.
5. Bottasso, C. L., Chang, C.S., Croce, A., Leonello, D. and Riviello, L., "Adaptive Planning and Tracking of Trajectories for the Simulation," *Computer Methods in Applied Mechanics and Engineering*, vol. 195, (50-51), pp. 7052-7072, 2006.
6. Garcia, R. D., Valavanis, K. P. and Kandel, A., "Autonomous Helicopter Navigation During A Tail Rotor Failure Utilizing Fuzzy Logic," Mediterranean Conference on Control and Automation, Athens, 2007.
7. Budiyono, A. and Wibowo, S. S., "Optimal Tracking Controller Design for a Small Scale Helicopter," *Journal of Bionic Engineering*, vol. 4, (4), p. 271−280, 2007.
8. Abbeel, P., Coates, A., Hunter, T. and Ng, A. Y., "Autonomous Autorotation of an RC Helicopter," Experimental Robotics: The Eleventh International Symposium, 2008.
9. Arslan, Y. O., Okcu, I. D. and Yavrucuk, I., "Flight Path Generation for a Helicopter in Tail Rotor Failure Condition," 48th European Rotorcraft Forum, Winterthur, Switzerland, September 6-8, 2022.
10. Operator's Manual for UH-60A, UH-60L and EH-60A Helicopters, Headquarters, Department of the Army, Washington, D.C., 1996.

11. S. Avcıoğlu, Controller Design and Simulation for A Helicopter During Target Engagement, MSc. Thesis, Middle East Technical University, 2011.

12. S. Das and K. Halder, "Missile Attitude Control via a Hybrid LQG-LTR-LQI Control Scheme with Optimum Weight Selection," in First International Conference on Automation, Control, Energy and Systems (ACES), Adisaptagram, 2014.

13. J. V. R. Prasad, A. J. Calise, Y. Pei and J. E. Corban, "Adaptive Nonlinear Controller Synthesis and Flight Test Evaluation on An Unmanned Helicopter," in IEEE International Conference on Control Applications, Kohala Coast, 1999.

14. O. Tarımcı, Adaptive Controller Applications for Rotary Wing Aircraft Models of Varying Simulation Fidelity, MSc. Thesis, Middle East Technical University, 2009.

15. R. L. Williams II and D. A. Lawrence, Linear State-Space Control Systems, John Wiley & Sons, Inc., 2007.